Journal of Inorganic and Organometallic Polymers and Materials (2021) 31:3842–3856
https://doi.org/10.1007/s10904-021-02019-9

Enhanced Thermal Stability and Flame Retardancy of Poly(Vinyl Chloride) Based Composites by Magnesium Borate Hydrate-Mechanically Activated Lignin

Wuxiang Zhang[1] · Haoran Wu[1] · Nan Zhou[1] · Xiunan Cai[1] · Yanjuan Zhang[1] · Huayu Hu[1] · Zhenfei Feng[2] · Zuqiang Huang[1] · Jing Liang[1]

Received: 22 February 2021 / Accepted: 3 May 2021 / Published online: 7 May 2021

Abstract

To improve the thermal stability and flame retardancy of poly(vinyl chloride) (PVC) based composites, magnesium borate hydrate-mechanically activated lignin (MBH-MAL) complex was in-situ synthesized by hydrothermal method for using as a novel additive. In addition, MBH-lignin (MBH-L) complex, MAL, MBH, and common mixing of MBH and MAL (MBH+MAL) were also prepared for comparative investigation. MBH-MAL showed synergistic improving effect on PVC as MBH-MAL/PVC composite exhibited excellent thermal stability and flame retardancy. The static thermal stability time was 871 s and limit oxygen index was 32.54%, indicating that MBH-MAL effectively inhibited the generation of HCl from thermal decomposition of PVC and prevented the combustion of PVC based composites in air. MBH-MAL/PVC composite still exhibited outstanding tensile and flexural properties. Moreover, the enhancing mechanism of MBH-MAL on the thermal stability and flame retardancy of PVC based composites was proposed.

Graphic Abstract

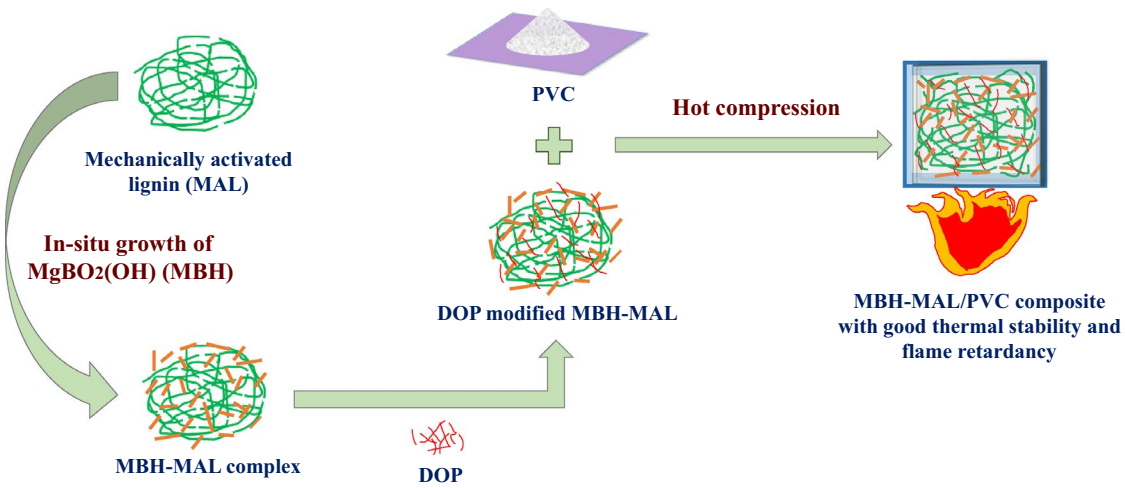

Keywords Polymer-matrix composites · Lignin · Magnesium borate hydrate · Thermal properties · Flame retardancy

✉ Yanjuan Zhang
zhangyj@gxu.edu.cn

[1] School of Chemistry and Chemical Engineering, Guangxi University, Nanning 530004, China

[2] School of Mechanical Engineering, Guangxi University, Nanning 530004, China

1 Introduction

Poly(vinyl chloride) (PVC), a typical thermoplastic polymer, is widely used in many fields because of its unique properties, especially good corrosion resistance and mechanical properties [1–5]. A certain amount of plasticizers is added to facilitate the manufacture of flexible PVC, which inevitably reduces the flame retardancy of PVC based composites [6]. Dioctyl phthalate (DOP), with the properties of low volatility, suitable softness, good heat resistance and weatherability, is commonly used as an efficient plasticizer to improve the processability of PVC [7]. DOP can also help to enhance the dispersion of additives in the manufacture of various PVC based functional composites [8]. However, when the composites are burned, both plasticizer and PVC decompose due to poor thermal stability, releasing complex gases that are harmful to human health [9, 10]. It is crucial to develop an environmentally friendly additive that can improve the thermal stability and flame retardancy of PVC based composites [11].

Borate hydrate, a new type of inorganic flame retardant, is considered as an efficient fire protection and safety flame retardant system for polymers ascribed to the high thermal stability, low cost [12], and smoke suppression performances [13]. When borate hydrate is used as flame retardant for PVC, metal ions can promote the release of HCl (gas flame retardant) and the formation of char (preventing the transfer of oxygen and heat) at high temperature, and part of the borate roots can form a glass layer on the surface of char to stabilize it [14]. Additionally, the resulting HCl molecules interact with borate to produce H_2O molecules, which further reduce heat loss and harmful gases generated from thermal decomposition of PVC. However, hydrophilic inorganic particles difficultly disperse well in polymers. It is of great significance to improve the interfacial compatibility between borate hydrate and PVC and simultaneously increase the properties of PVC.

Lignin contains a large number of phenolic hydroxyl, alcohol hydroxyl, carbonyl, methoxyl, and carboxyl groups [15, 16]. The interaction between lignin and PVC can be proved to be a "proton donor-proton receptor". Theoretically, hydrogen bonds can be formed between the α-hydroxyl groups of lignin and the chlorine of PVC, or between the carbonyl groups of lignin and the α-hydrogen of PVC [17, 18]. In addition, lignin has a complex structure composed of cross-linked 3D networks, contributing to excellent compatibility with PVC [19]. In native state, lignin has a low glass-to-rubber transition temperature and is part of a block copolymer with non-crystalline polysaccharides [20]. The phenolic hydroxyl groups can trap free radicals due to the stereoscopic hindrance, so lignin can be a heat stabilizer to hinder free radical reactions in the process of PVC pyrolysis [21]. Specially, lignin can be also used as an flame retardant due to that a large amount of char formed during the combustion of lignin can act as an insulating layer on the surface of the combustion material, which prevents the diffusion of oxygen and heat, as well as the volatilization of degradation products [22, 23]. It is worth mentioning that the metal ions in the borate hydrate and the electronegative lignin have a strong interaction effect [24]. Suitable combination of borate hydrate and lignin as an additive can promote the compatibility between PVC and polar borate hydrate, which is expected to reduce the damage to the mechanical properties of PVC based composites while improving its thermal stability and flame retardancy.

To improve the interaction between lignin and borate hydrate, an efficient pretreatment for lignin is important to enhance its activity. Mechanical activation (MA), referring to the use of mechanical actions to change the structure and physicochemical properties without any reagents, is considered to be an effective, convenient, and environmentally friendly method [25]. The aggregation structure of lignin can be loosen by MA pretreatment and lead to the oxidation of oxygen-containing groups and the generation of aldehyde, ketone, or carboxyl groups [26], contributing to the increase in its reactivity with other polar materials and uniform dispersion in the polymer matrix [27].

In this paper, mechanically activated lignin (MAL) was added to the reaction system of magnesium borate hydrate (MBH) for in-situ synthesis of MBH-MAL complex, which was used as heat stabilizer and flame retardant for PVC. MBH-lignin (MBH-L) complex, MBH, MAL, and common mixing of MBH and MAL (abbreviated as MBH+MAL) was also prepared for comparative investigation. The thermal stability, flame retardancy, and mechanical properties of PVC based composites with different additives were comparatively studied to confirm the reinforcing effect of MBH-MAL. Based on the investigation of the properties of the composites and characterizations of the additives and composites, the enhancing mechanism of MBH-MAL on the thermal stability and flame retardancy of PVC based composites was proposed. This study can provide a new insight into the development of a novel inorganic–organic complex additive for improving the properties of PVC based composites.

2 Experimental

2.1 Materials

PVC (S65 type, k value: 64.6–66.0) was purchased from Formosa Plastics Industry Co., Ltd. (China). Enzymatic

lignin was purchased from Jinan Yanghai Chemical Co., Ltd. (China). DOP (99%) was provided by Shandong Yousu Chemical Technology Co., Ltd. (China). $Na_2B_4O_7{\cdot}10H_2O$, $NH_3{\cdot}H_2O$, and $MgCl_2{\cdot}6H_2O$ (analytical grade) were purchased from Chengdu Fushan Chemical Reagent Co., Ltd. (China). Absolute ethanol (analytical grade) was supplied by Xiqiao Science and Technology Co., Ltd. (China). All chemicals were used without further purification. Deionized water was used throughout the experiment where required.

2.2 Preparation of MAL, MBH, MBH+MAL, MBH-MAL, and MBH-L

MAL was prepared in a customized stirring ball mill [21]. 25 g of dried lignin and 400 mL of zirconia milling balls (5 mm diameter) were added to a jacketed stainless steel tank (1200 mL). Lignin was subjected to dry milling at a speed of 450 rpm under a constant temperature of 50 °C. After milled for different MA time (30, 60, or 90 min), the balls were removed from the mixture by a sieve, and the resulting sample was MAL.

MBH was prepared as follows [28]: 20.43 g of $Na_2B_4O_7{\cdot}10H_2O$ was dissolved in 100 mL of water (60 °C). 100 mL of 1.5 $mol{\cdot}L^{-1}$ $MgCl_2$ solution was placed in a 500 mL beaker, and 60 mL of 6.5 $mol{\cdot}L^{-1}$ ammonia aqueous was slowly added with magnetic stirring. Then, the $Na_2B_4O_7$ solution was added. The prepared mixture was put into an autoclave to react at 190 °C under a pressure of 2 MPa with a mechanical stirring of 300 rpm. After 7 h of reaction, the mixture was treated by a repeated washing-filtration process with deionized water until the filtrate was neutral, and ethanol was used for the last washing-filtration process. After dried to constant weight at 120 °C, MBH ($MgBO_2(OH)$) was obtained.

MBH+MAL was prepared by mixing MBH and MAL at room temperature by a high-speed mixer (10,000 rpm, Tester FW80, China) with the mass ratio of 1:1.

In-situ synthesis of MBH-MAL and MBH-L was performed in the preparation process of MBH. After mixing $MgCl_2$ solution and ammonia aqueous, MAL or native lignin was added to the mixed solution, and $Na_2B_4O_7$ solution was finally added (mass ratio of MAL (or lignin) to MBH was 1:1). This mixture was put into the autoclave for reaction under the same conditions as the preparation of MBH. After the same treatment, MBH-MAL and MBH-L were obtained.

2.3 Preparation of PVC Based Composites

DOP (20 g in a batch) and MBH-MAL (or other prepared additives, with 0, 5, 10, 15, 20, or 25 g in a batch) were uniformly mixed, and then the mixture was put in an oven at 120 °C for 60 min. Add PVC to the mixture (for each batch, the total mass of PVC and additive was 100 g), the resulting mixture was again put in the oven at 80 °C for 90 min. The mixture was placed in a two-track internal mixer (Helite XK-300, China) to obtain a uniformly mixed sheet. The sheet was compression-molded in a flat vulcanizer (Shuangli XLB25-D, China) for 15 min at 185 °C under a pressure of 8 MPa. After cooled to room temperature, the resulting PVC based composites were obtained. The entire preparation process of MBH-MAL/PVC composites is shown in Fig. 1.

2.4 Measurement of Static Thermal Stability by Congo Red Method

According to GB/T 2917.1-2002 (China), the static thermal stability of the composites was tested by the Congo red method [21, 29]. The prepared composites were pulverized into granules (particle size of 10−14 mesh). In static air, the composite granules were placed in a flat-bottom test tube with a height of 50 mm and Congo red test strip was placed 25 mm above it. The testing was maintained at 180 °C, and the time for the upper Congo red test paper changing to blue (equivalent to pH = 3) caused by the HCl gas generated from thermal

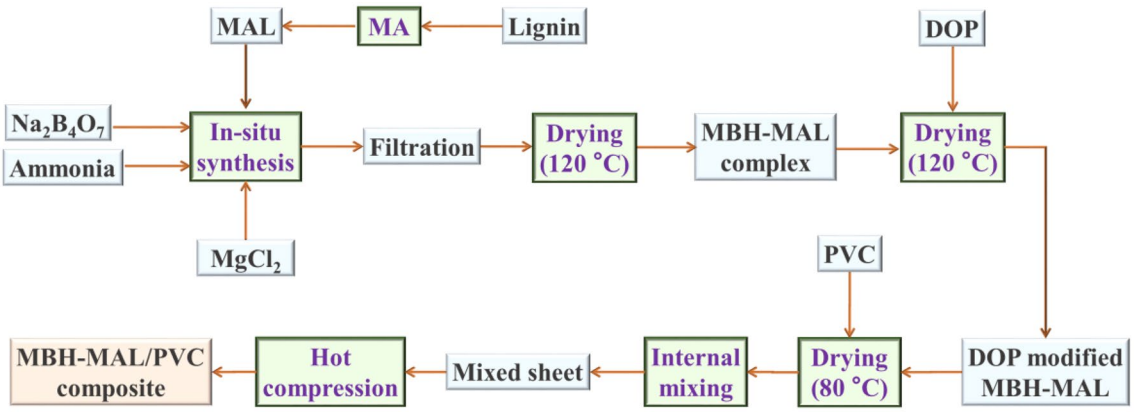

Fig. 1 Preparation process of MBH-MAL/PVC composites

decomposition of PVC was recorded as static thermal stability time [30]. The measurements were carried out at least in triplicate, and the data were statistical average values.

2.5 Measurement of Mechanical Properties

Mechanical properties of the prepared composites were measured by an MWW-20A universal testing machine (Jinan Tianchen Testing Machine Manufacturing Co., Ltd, China). The tensile strength of the specimens (100 × 20 × 4 mm) were measured at a crosshead speed of 2.0 mm·min^{-1} in accordance with GB/T1040-2006 (China) at 25 °C [31]. The flexural strength of the specimens (100 × 10 × 4 mm) was measured by a three-point flexural test at a crosshead speed of 1.0 mm·min^{-1} according to GB/T 9341–2008 (China) at 25 °C [31]. The measurements were performed at least in triplicate to obtain statistical average values.

2.6 Characterizations

The crystal structure of the samples was determined by X-ray diffraction (XRD) on a D/MAX 2500 V diffractometer (Rigaku, Japan) using Cu Kα radiation (λ = 0.154 nm) at 40 kV and 30 mA, recorded from 5° to 80° with a scanning speed of 10°·min^{-1}. The morphology and microstructure were observed by an S-3400 N scanning electron microscope (SEM, Hitachi, Japan) with an accelerating voltage of 5 kV and a working distance of 6.5 mm [32]. Energy dispersive spectroscopy (EDS) elemental maps were obtained by energy dispersive X-ray analysis using a Hitachi S-3400 N energy dispersive spectrometer. The chemical structure of the samples was characterized by Fourier transform infrared spectroscopy (FTIR) on a FTIR-8400S spectrometer (Shimadzu, Japan) with a resolution of 4 cm^{-1} and a recording frequency range of 400−4000 cm^{-1}. Thermogravimetric analysis (TGA) was carried out using a Q50 thermogravimetric analyzer (TA Instruments, USA). A sample of about 5 mg was weighed into an aluminum crucible and heated to 600 °C at a heating rate of 20 °C·min^{-1} under the protection of air. The hydrophobicity of the samples was tested by a DSA-100 Lukes Contact Angle Gauge (KRUSS, Germany) with a water droplet volume of 3 μL and a water droplet residence time of approximately 20 s. The flame retardant properties of the samples was determined by a JF-3 limiting oxygen chamber (Jiangning, China) with gas velocity of 10 L·min^{-1} and gas purity of 99.99 vol%.

3 Results and Discussions

3.1 Characterizations of the Prepared Additives

The microstructures of the prepared MBH, MBH-L, and MBH-MAL additives were characterized by XRD and SEM, and the results are shown in Fig. 2. In the XRD pattern of MBH (Fig. 2a), the appeared diffraction peaks corresponded to (110), (020), (200), (220), (230), (320), (330), (410), (311), (141), (500), (160), and (022) planes of $MgBO_2(OH)$, indicating that $MgBO_2(OH)$ was successfully synthesized by hydrothermal method. In the XRD patterns of MBH-L and MBH-MAL, most of the characteristic diffraction peaks of $MgBO_2(OH)$ became weak but the intensity of the (110) peak increased as the presence of lignin. Lignin is an amorphous polymer without crystal structure but is rich in −OH and −COOH groups. During the formation of $MgBO_2(OH)$ with adding lignin, Mg^{2+} bonded with −COOH and $[BO_2(OH)]^{2-}$ bonded with −OH, contributing to the in-situ growth of MBH in the lignin network [33]. In addition, MA pretreatment led to the increase of active −OH and −COOH groups in lignin, which could result in stronger bonding between MAL and MBH. As most of MBH were submerged into lignin, the characteristic diffraction peaks of $MgBO_2(OH)$ in the XRD patterns of MBH-L and MBH-MAL were weaker and wider compared with those in the pure MBH. The enhancement of (110) peak could be due to an increased content of −OH groups, especially in MBH-MAL. These can prove that the synthesized MBH-L and MBH-MAL contained $MgBO_2(OH)$.

The microscopic structure of these samples could be visually observed by SEM analysis. As presented in Fig. 2b, MBH consisted of needle-like nanocrystalline whiskers with a length of about 2 μm and flakes. The MBH crystals in MBH-L were flaky and embedded in the lignin network (Fig. 2c). During the in-situ synthesis of MBH-L, the hydroxyl groups in lignin could combined with MBH in the form of hydrogen bonds, contributing to the change of the morphology of MBH in MBH-L compared with pure MBH. Furthermore, the morphology of MBH in MBH-MAL (Fig. 2d) shows greater change, ascribed to that more active −OH and −COOH groups in MAL had a greater impact on the growth of MBH whiskers. Therefore, the MBH crystal whiskers in MBH-MAL complex were smaller and embedded in the MAL network.

The changes in functional groups and chemical structure of different samples were characterized by FTIR. As shown in Fig. 3, characteristic absorption peaks attributed to lignin aromatics skeleton (1598, 1511, 1460, and 1422 cm^{-1}), −OH stretching vibration (3414 cm^{-1}), C–H stretching vibration (2937 cm^{-1}), CH_2 vibration (2847 cm^{-1}), and C=O stretching of carbonyl groups (1702 cm^{-1}) can be clearly observed in the FTIR spectra of lignin [34, 35], and MA did not destroy the basic skeleton structure of lignin. After 60 min of MA, the absorption peak of the stretching vibration of aromatic and aliphatic −OH groups moved from 3421 to 3435 cm^{-1}, indicating that MA increased the hydrogen bond energy and led to the increase of free hydroxyl groups and the reactivity of lignin [36]. In the spectrum of MBH, the strong absorption

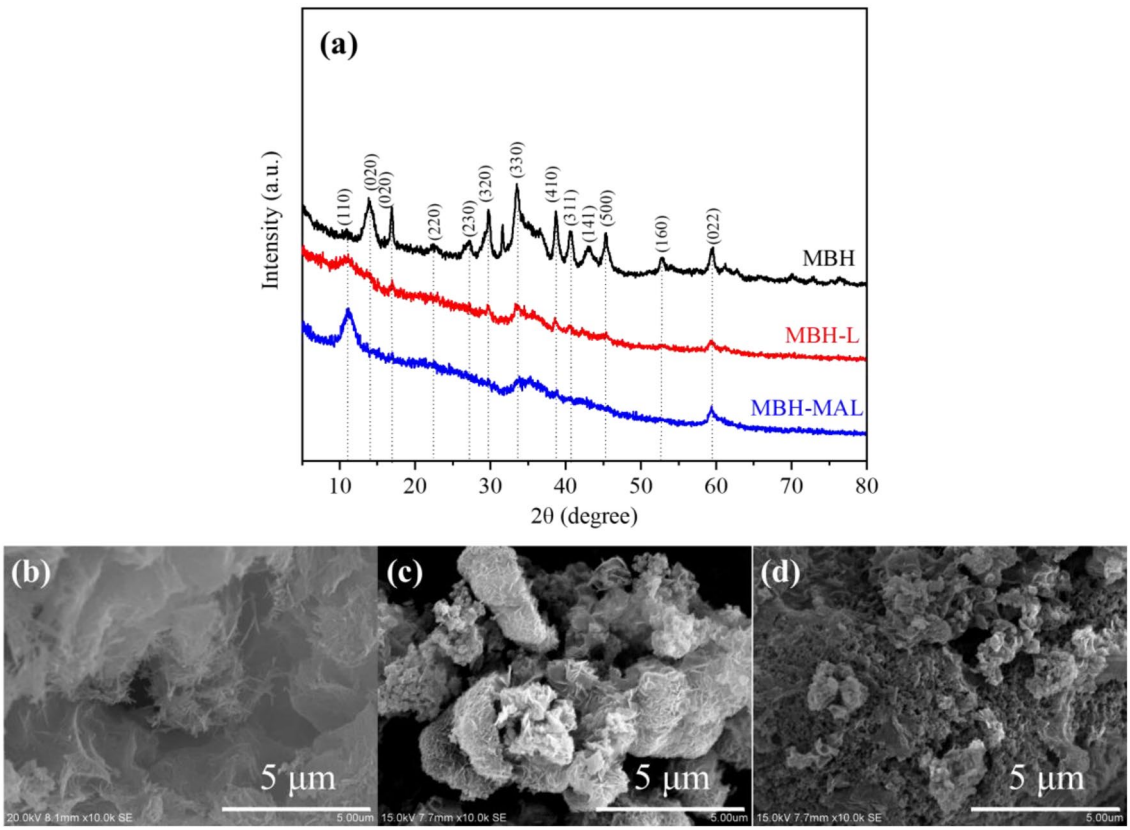

Fig. 2 (**a**) XRD patterns of different samples; SEM images of (**b**) MBH, (**c**) MBH-L, and (**d**) MBH-MAL

peak at 3452 cm^{-1} was the stretching vibration of hydroxyl groups; the peak at 1620 cm^{-1} was the characteristic absorption of bound water; the antisymmetric telescopic vibrations of $B_{(3)}$−O were related to the peaks at 1489 and 1364 cm^{-1}; the peaks at 1000 and 921 cm^{-1} were symmetrical retractable vibration of $B_{(3)}$−O; the peaks at 1282 and 1209 cm^{-1} were the flexural vibration in the surface of B–O–H; the peak at 536 cm^{-1} was the flexural vibration of $B_{(3)}$–O; the peaks at 707 and 623 cm^{-1} were extra-plane curved vibration of $B_{(3)}$–O; the peak at 497 cm^{-1} was the stretching vibration of Mg–O bonds [37]. FTIR analysis also confirmed the successful synthesis of $MgBO_2(OH)$. The FTIR spectra of MBH-L and MBH-MAL show the characteristic adsorption peaks of lignin and MBH. The absorption peak of –OH groups shifted to a lower wavenumber compared with that of lignin and MAL (from 3421 and 3435 cm^{-1} to 3416 and 3422 cm^{-1}, respectively), implying a strong evidence for the interaction between the hydroxyl groups of lignin and MBH via in-situ synthesis.

3.2 Effect of DOP on Hydrophobicity of the Prepared Additives

DOP is commonly used as plasticizer for PVC. In this study, the prepared additives were firstly mixed with DOP for modification, and then the mixture was added to PVC for further processing. The change in the chemical structure of MBH before and after mixed with DOP was characterized by FTIR, and the effect of DOP on the hydrophobicity of MBH, MBH-L, and MBH-MAL was evaluated by water contact angle characterization (the DOP-modified samples used for characterizations were washed with CCl_4 to remove the unbound DOP). As shown in Fig. 4a, the band at 2853 cm^{-1} was related to the characteristic adsorption of C–H bonds in the long carbon chain of DOP. The peaks at 766 and 740 cm^{-1} were the benzene ring adjacent double replacement part of the single bond vibration. The peak at 1724 cm^{-1} was due to the expansion vibration of C=O of ester. The bands at 1462, 1271, and 1116 cm^{-1} were caused by the characteristic adsorption of −C–O–C− vibration. The characteristic peaks of MBH are all presented in the spectrum of DOP-modified MBH, but the peak type was significantly blunt. The DOP with long chains dispersed in MBH and reduced the crystallinity of MBH.

As shown in Fig. 4b, the water contact angles of MBH, MBH-L, and MBH-MAL increased by 27.8, 12.4, and 12.8% respectively after modified with DOP, and DOP-modified MBH-MAL exhibited the highest water contact angle (68.5°). DOP with two hydrophobic chains could

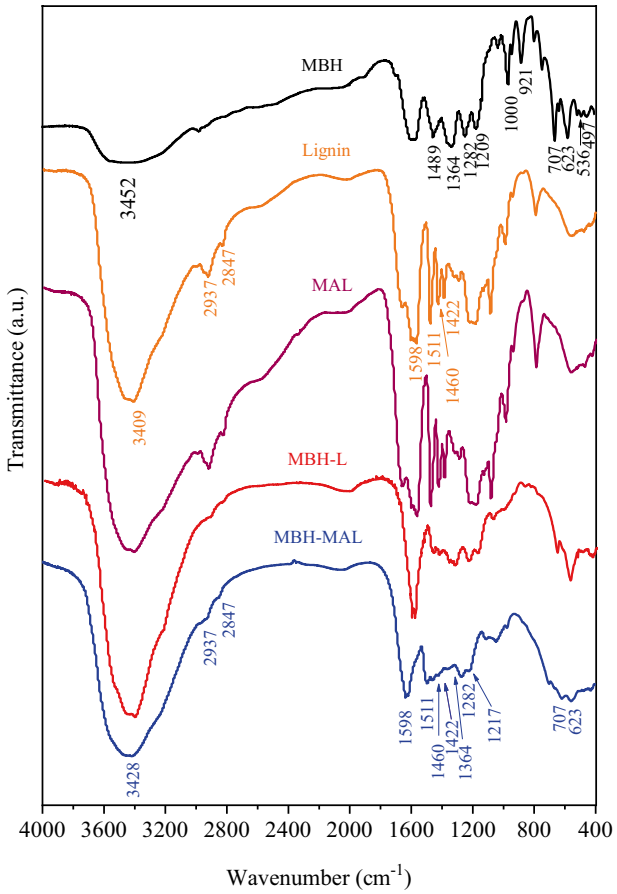

Fig. 3 FTIR spectra of different samples

embed into MBH, increasing the hydrophobicity and dispersity of MBH and its complex. The increase in the hydrophobicity of MBH, MBH-L, and MBH-MAL additives modified with DOP could significantly improve their compatibility with PVC.

3.3 Effect of Different Additives on Static Thermal Stability of the Composites

Static thermal stability testing was to evaluate the inhibition of additives for HCl generated from thermal decomposition of PVC, and longer static thermal stability time means better inhibition effect. The effect of different additives on the static thermal stability of PVC based composites is shown in Table 1. To explore the effect of the addition amount of additives on the static thermal stability of the composites, different amounts of MBH and MBH-L were added to PVC for comparative study. In addition, lignin with different MA time was used to prepare MBH-MAL to determine the effect of MA time on the static thermal stability of MBH-MAL/PVC composites. The static thermal stability of pure PVC was poor, and the test result of Congo red was only 147 s, but that of the composites gradually improved as increasing the addition amount of MBH. The static thermal stability of the composites with adding 15 wt% of MBH or MBH-L increased by 69 or 390% compared with that of pure PVC. For using MBH-MAL as additive, the static thermal stability of MBH-MAL/PVC composites improved as the increase of MA time. The static thermal stability of MBH-MAL/PVC composite with MA time of 60 min was 15.6% higher than that of MBH-L/PVC composite. The addition amount of 15 wt% for all additives in PVC based composites and MA time of 60 min for lignin were chosen for further investigations.

Figure 5 shows that the static thermal stability of MAL/PVC composite was 85.7% higher than that of pure PVC, which might be due to the enhancement of MAL as a rigid particle, and MA reduced the particle size of lignin to promote its dispersion and improve the compatibility with PVC

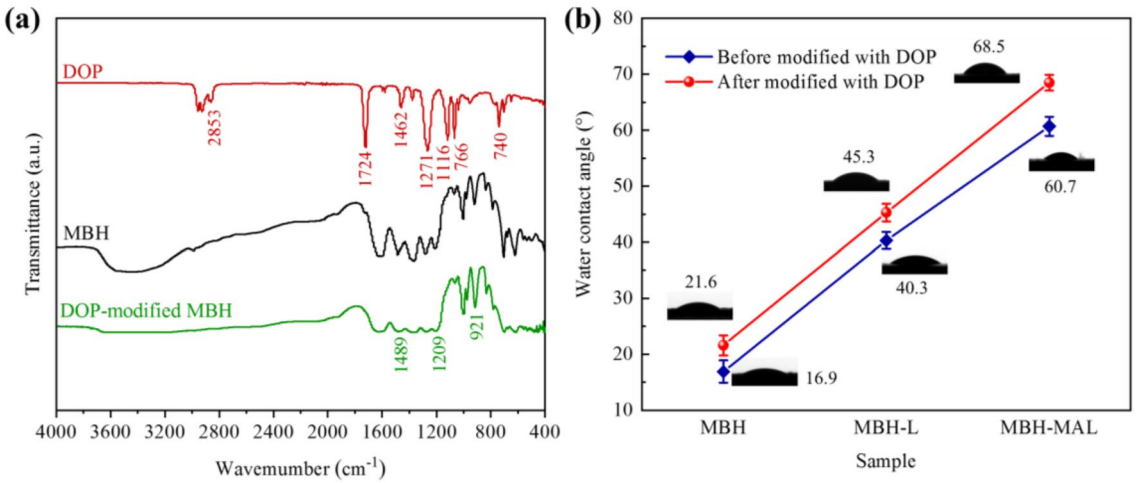

Fig. 4 (**a**) FTIR spectra of DOP, MBH, and DOP-modified MBH; (**b**) water contact angle of the samples before and after modified with DOP

Table 1 Static thermal stability of PVC, MBH/PVC, MBH-L/PVC, and MBH-MAL/PVC composites

Sample	Amount of additive (wt%)	MA time (min)	Thermal stability time (s)
PVC	0	–	147 ± 6
MBH/PVC	5	–	169 ± 7
	10	–	191 ± 8
	15	–	249 ± 10
	20	–	284 ± 9
	25	–	342 ± 7
MBH-L/PVC	5	0	385 ± 10
	10	0	452 ± 12
	15	0	720 ± 14
	20	0	774 ± 11
	25	0	818 ± 13
MBH-MAL/PVC	15	30	783 ± 14
	15	60	832 ± 15
	15	90	847 ± 12

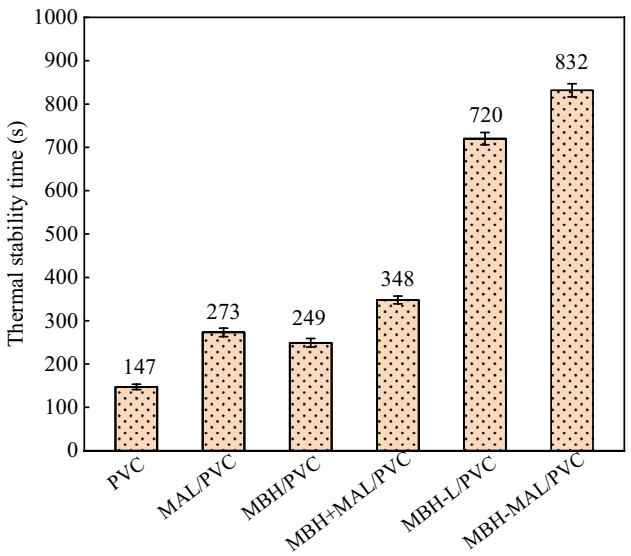

Fig. 5 Static thermal stability of different PVC based composites (amount of additive = 15 wt%; MA time = 60 min)

matrix. The static thermal stability of MBH/PVC composite was only slightly higher than that of pure PVC. MBH is a hydrophilic crystal material and could severely aggregate in PVC matrix, failing to play a role in improving the thermal stability of the composite. The static thermal stability of MBH+MAL/PVC composites was improved compared to that of MBH/PVC composite, attributing to the three-dimensional structure and thermal stability of MAL. This is owing to that MAL improved the static thermal stability of PVC, and the three-dimensional mesh structure of MAL had an effect on preventing the aggregation of MBH. It is worth noting that the static thermal stability of MBH-L/PVC and MBH-MAL/PVC was 100.1% and 139.1% higher than that of MBH+MAL/PVC, respectively. Firstly, in-situ synthesis of MBH-L and MBH-MAL complex at high temperature and pressure contributed to the growth of MBH whiskers into the skeleton and network of lignin, preventing the agglomeration of MBH with a certain hydrophobicity. Secondly, the good dispersion of MBH-L and MBH-MAL in the composites could lead to strong interaction with PVC, inhibiting the generation of HCl from the thermal decomposition of PVC.

3.4 Effects of Different Additives on Thermal Degradation Properties of the Composites

Figure 6 and Table 2 show the thermogravimetric analysis results of different PVC based composites. After excluding the thermal decomposition residues of MBH and L, the residual char content of the sample is the residual char data after PVC combustion. As revealed from the TGA curves in Fig. 6a, the degradation of different PVC based composites can be divided into two stages. The first decomposition occurred in a temperature range of 250–350 °C attributed to the loss of HCl originated from chlorine (Cl) radicals from −C–Cl bonds and hydrogen radical from adjacent C–H groups [38]. In addition, the thermal decomposition of DOP also occurred at this stage. The second decomposition occurred in a temperature range of 400–520 °C, which might be due to the degradation of polyene backbones [38]. Pure PVC had a mass loss of 65% in the first stage, ascribing to the decomposition stage of the main body of PVC, and also a stage that needs to be focused on improving the thermal stability of PVC. In addition, the maximum weight loss rate of MBH/PVC composite occurred at a lower temperature than pure PVC, but the residual char content (12.4%) of MBH/PVC composite was higher than that of pure PVC (11.9%). MBH lost its water at high temperature, which took away a lot of heat. Part of MBH formed a glassy expansion coating, which facilitated the carbonization of composites and prevented the entry of oxygen. Simultaneously, HCl released from PVC and Mg^{2+} in MBH combined to form $MgCl_2$. Temperature in maximum thermal decomposition rate (T_{max}) of pure PVC was 294 °C. T_{max} of MBH-L/PVC and MBH-MAL/PVC were 5 and 10 °C higher than pure PVC, respectively, which was consistent with the results of static thermal stability. Compared with the previously reported PVC based composites [39, 40], MBH-MAL/PVC exhibited a higher T_{max}. The removal of HCl is generally believed to be caused by oxygen free radicals in the air [41], while the H atom free radicals given by phenol in lignin can combine with the degraded PVC macromolecular free radicals to form the substances that cannot react with O_2, thus forming a thermal stabilization effect [21]. MA reduced the particle size of lignin and increased the surface phenol content, which

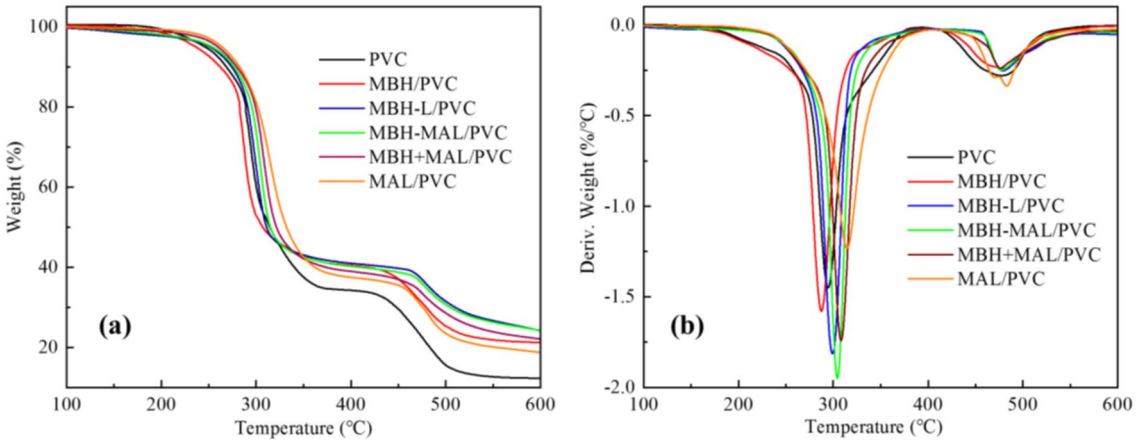

Fig. 6 (**a**) TGA and (**b**) DTG curves of different PVC based composites (amount of additive = 15 wt%, MA time = 60 min)

Table 2 The actual char residue of the composites

Sample	Char residue (%)
PVC	11.9
MBH/PVC	12.4
MBH-L/PVC	17.4
MBH-MAL/PVC	17.9
MBH+MAL/PVC	15.6
MAL/PVC	13.7

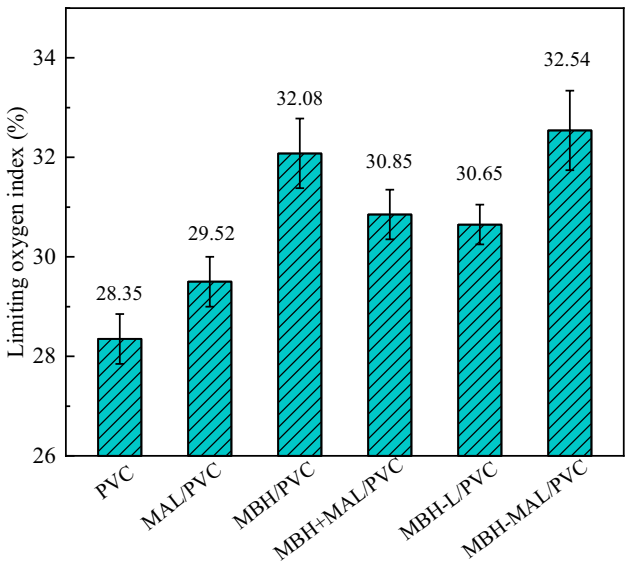

Fig. 7 LOI of different PVC based composites (amount of additive = 15 wt%, MA time = 60 min)

resulted in a high char residue of 17.9% for MBH-MAL/PVC composite. The char residue of MBH-MAL/PVC composite was higher than that of the PVC based composites reported in previous literature [39]. The char content of MBH+MAL/PVC composite was 12.8% lower than that MBH-MAL/PVC composite as MBH, MAL and PVC were mutually dispersed via common mixing, which could not bind the thermal decomposition of PVC. In the first stage, MAL/PVC composite could effectively restrain the escape of HCl, so its maximum weight loss rate occurred at the highest temperature. However, the char residue of MAL/PVC composite was only 13.7% for lacking of co-action between PVC and MBH.

3.5 Effect of Different Additives on Flame Retardancy of the Composites

The effect of different additives on the flame retardancy of PVC based composites was measured by limit oxygen index (LOI) and the observation of combustion process, and the results are shown in Figs. 7 and 8. The LOI of MAL/PVC composites was only 4.1% higher than that of pure PVC (28.35%), revealing that single MAL had a weak effect on the flame retardancy performance of the composites. The LOI of MBH/PVC was 13.2% higher than that of pure PVC, indicating that MBH had a significant effect on improving the flame retardancy of PVC based composites, which is consistent with the results of static thermal stability. The LOI of MBH+MAL/PVC composites was 4.6% higher than MAL/PVC, which is consistent with the results of static thermal stability. The thermal stability of MBH-L/PVC composite was similar to that of MBH/PVC composite, but the flame retardancy performance of MBH-L/PVC composite was worse than that of MBH/PVC composite. The LOI of MBH-L/PVC composite was 8.1% higher than that of pure PVC and 4.5% lower than that of MBH/PVC composite, for the MBH content in MBH-L/PVC composite was only half of that in MBH/PVC composite. The LOI of MBH-MAL/PVC composite was 14.8 and 6.2% higher than that of pure

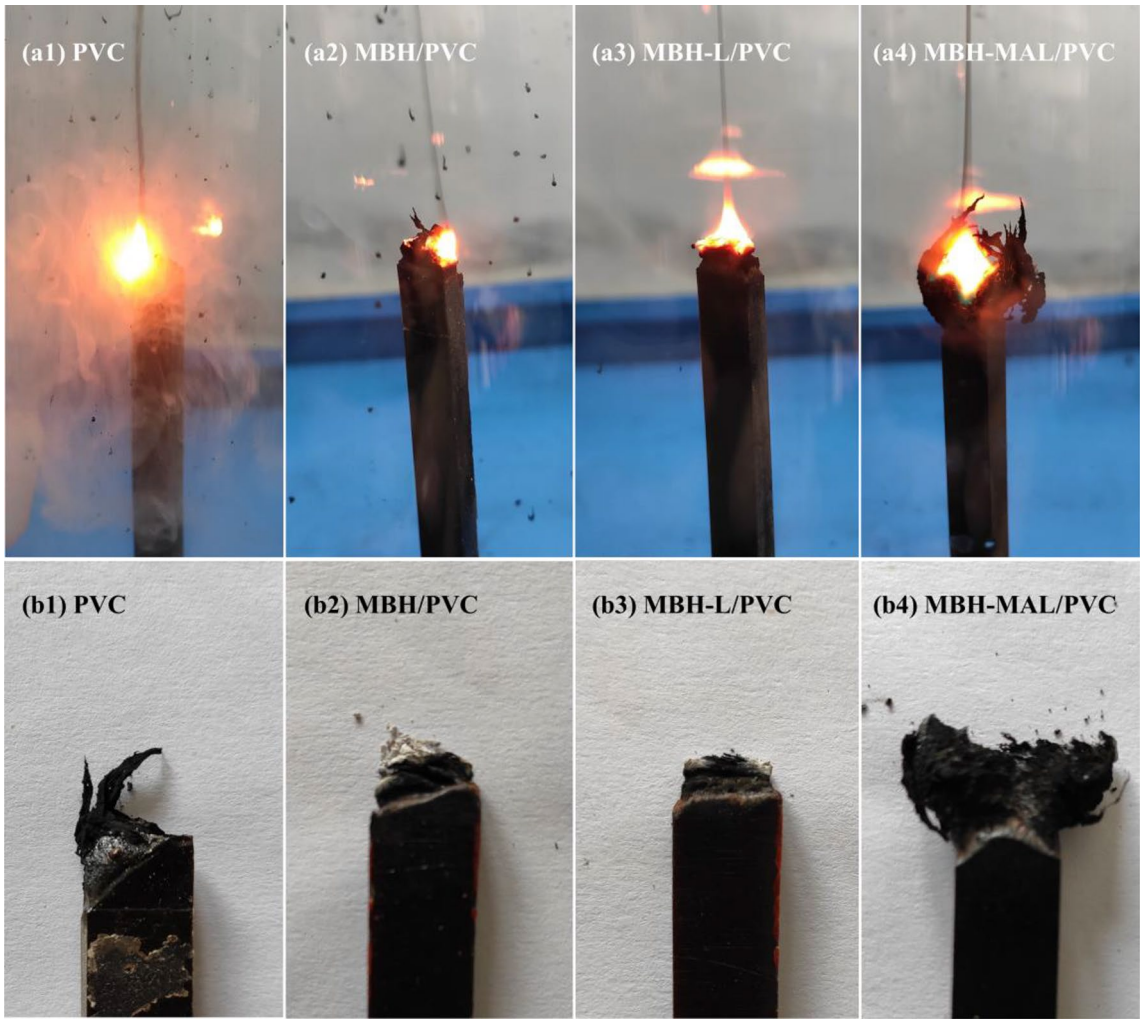

Fig. 8 Photos of (**a**) combustion phenomena and (**b**) combustion residues of different PVC based composites (amount of additive = 15 wt%, MA time = 60 min)

PVC and MBH-L/PVC composites, respectively, and higher than that of the previously reported PVC based composites [42, 43], showing that MA was benefit to improving the flame retardancy of PVC based composites. These results demonstrate that both MBH and lignin could improve the flame retardancy of PVC based composites, especially the additives prepared by in-situ synthesis with MA-pretreated lignin. The flame retardancy performance of the composites was improved with the addition of MBH-MAL, and the LOI of MBH-MAL/PVC composite reached the highest value of 32.54%, implying the synergistic effect of MBH and MAL. During the combustion process, MBH formed a glassy expansion coating that hindered the escape of volatile combustible materials and the entry of oxygen, enhancing the tight structure of char [13]. In addition, MBH was dehydrated at high temperature and exhibited the endothermic and cooling effects [13]. A large amount of char formed from the carbonization of lignin during combustion acted as an insulating layer on the surface of the combustion material, which prevented the diffusion of oxygen and heat and the volatilization of degradation products [44]. The additives prepared by in-situ synthesis (especially MBH-MAL) exhibited excellent structure and properties, which help to significantly improve the flame retardancy of the PVC based composites.

Figure 8 presents the burning state and the shape of the combustion residues of PVC based composites during the LOI test. Pure PVC produced a large amount of white smoke when burning, and a large amount of black ash surrounded the flame, attributing to the decomposition products of PVC and DOP, which could not be burned completely and were carried out by HCl (Fig. 8a1). The glassy coating formed from MBH on the surface of the composites effectively prevented the release of toxic smoke, which led to the absence of white smoke during the burning of MBH/PVC, MBH-L/PVC, and MBH-MAL/PVC composites (Fig. 8a2–a4), and

the combustion residues further proved this result (Fig. 8b). MBH/PVC, MBH-L/PVC, and MBH-MAL/PVC composites had white residues after combustion (Fig. 8b2–b4), which were the residual MgO generated from the decompose of MBH at high temperature. There was still a lot of black ash around the flame of MBH/PVC composite (Fig. 8a2), which did not appear in the combustion of MBH-L/PVC and MBH-MAL/PVC composites. This proves that the additives containing lignin (especially MAL) could restrict the combustion of PVC based composites. The amount of MgO in MBH/PVC composite was more than that in MBH-L/PVC and MBH-MAL/PVC composites after burning, for the amount of MBH in MBH/PVC composite was twice of that in MBH-L/PVC and MBH-MAL/PVC composites. In fact, lignin (or MAL), MBH, and PVC formed an intumescent flame-retardant system at high temperature. PVC released HCl at high temperature to dilute the oxygen around the flame, and took away the heat (gas source). MBH formed a borate coating at high temperature to prevent the entry of oxygen and promote the PVC matrix to form char (acid source). Lignin is a natural polymer with extremely high carbon content, which became char at high temperature (carbon source). MA increased the activity of lignin, resulting in that the interaction in MBH-MAL was stronger than that in MBH-L. During the burning process, MAL and MBH promoted PVC to expand into char to reduce the release of black ash and toxic fumes, so MBH-MAL/PVC composite had fluffier and more combustion residues than MBH-L/PVC composite (Fig. 8b3, b4).

3.6 Effect of Different Additives on Mechanical Properties of the Composites

The effect of different additives on the mechanical properties of PVC based composites is shown in Fig. 9. The tensile and flexural strengths of pure PVC were 28.0 and 49.5 MPa, respectively, and those of the composites gradually reduced as increasing the addition amount of MBH. The tensile and flexural strengths of 15 wt% MBH/PVC composite reduced by 42.1 and 17.1% compared with those of pure PVC, respectively (Fig. 9a, b). After adding 5 wt% of MBH-L, the tensile strength of the composite decreased by 2%. With the increase of its content, the tensile strength of the composites no longer decreased significantly. Compared with MBH, the addition of equivalent amount of MBH-L had less negative effect to the tensile strength of PVC based composites. The flexural strength of 5 wt% MBH-L/PVC composite was 4.9% lower than that of pure PVC. With the increase of its content, the flexural strength of the composites slowly decreased. The flexural strength of 25 wt% MBH-L/PVC composite was 25% lower than that of pure PVC, which was 55% higher than that of 25 wt% MBH/PVC composite. With the increase of MBH content, the mechanical properties of the composites greatly reduced. The damage to the mechanical properties of the composites is due to the incompatibility of polar MBH and PVC. The mechanical properties of MBH-L/PVC composite were better than those of MBH/PVC composite, ascribed to that MBH was in-situ grown in the lignin network and the compatibility between MBH-L and PVC was improved, which effectively avoided the agglomeration of MBH in PVC matrix. The addition of these additives could destroy the uniform structure of PVC and thus the mechanical properties of these PVC based composites decreased as the increase in the addition amount of additives. On the contrary, the thermal stability and flame retardancy of the composites increased with the increase in the addition amount of additives. On the basis of comprehensive consideration, the optimum addition amount of additives was chosen to be 15 wt%, which could significantly improve the thermal stability and flame retardancy of the composites without significant decrease in their mechanical properties.

As shown in Fig. 9c, the tensile strength of MBH-MAL/PVC composites slowly increased as the increase of MA time. With MA time of 90 min, the tensile strength of MBH-MAL/PVC composite was 26.7 MPa, which increased by 4.9 and 64.4% compared with that of MBH-L/PVC and MBH/PVC composites, respectively. The flexural strength of MBH-MAL/PVC composites was maintained at about 40.8 MPa, indicating that MA time had no significant effect on the flexural strength of the composites. MAL has more active groups than lignin and is looser in structure, which allows it to bond better with MBH, so MBH bears more tensile stress in MBH-MAL/PVC composite. Comprehensively considering the effect of MA time on the mechanical properties, thermal stability, and flame retardancy of the composites, 60 min could be considered as an optimum MA time.

Figure 9d presents the effect of different additives on the tensile and flexural properties of PVC based composites. MAL had a great impact on the mechanical properties of the composites. In particular, the flexural strength of MAL/PVC composite reduced to almost half of that of pure PVC. MBH+MAL exacerbate the decrease trend of the mechanical properties of the composites. In contrast, the negative effect of MBH-L and MBH-MAL on the composites was weak, attributing to their special structure by in-situ synthesis. The tensile property of MBH-MAL/PVC was higher than that of the PVC based composites reported in previous studies [43, 45]. Firstly, the needle-like structure of MBH was responsible for the stress transfer during the fracture of the composites, which maintained the mechanical properties of the composites. Secondly, MBH was uniformly dispersed in lignin (or MAL) with better hydrophobicity to avoid aggregation, leading to satisfactory compatibility with PVC matrix. Therefore, the MBH-MAL complex prepared by in-situ synthesis could not only effectively enhance the

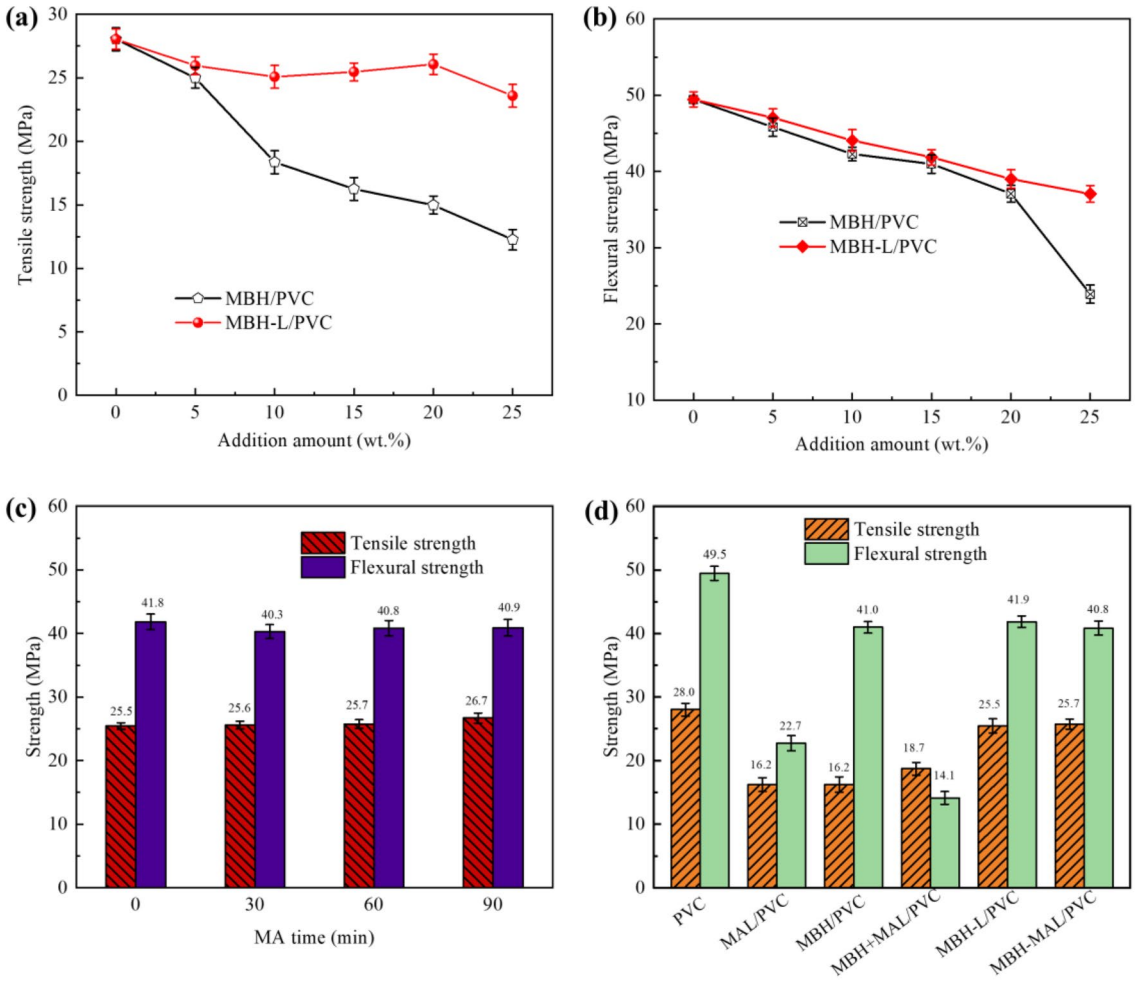

Fig. 9 (**a**) Tensile strength of MBH/PVC and MBH-L/PVC composites with different amount of additives; (**b**) flexural strength of MBH/PVC and MBH-L/PVC composites with different amount of additives; (**c**) tensile strength and flexural strength of MBH-MAL/PVC composites with different MA time (amount of additive = 15 wt%); (**d**) tensile strength and flexural strength of the PVC based composites with different additives (amount of additive = 15 wt%, MA time = 60 min)

thermal stability and flame retardancy of PVC based composites, but also had little effect on the mechanical properties of the composites.

3.7 SEM and EDS Analyses of the Composites

The influence of different additives on the microstructure of the fractured surface of PVC based composites was characterized by SEM, and the results are shown in Fig. 10. The cross-section of the pure PVC was very smooth with a layered fracture mark, indicating a brittle fracture (Fig. 10a). The cross-section of MAL/PVC composite was stacked in a layered manner along the vertical direction, which caused stress fracture in the direction of stretching (Fig. 10b). The agglomeration and accumulation of MBH in MBH/PVC composite was very serious (Fig. 10c). MBH was seriously agglomerated inside the composite, and the uneven dispersion of MBH in the PVC matrix led to uneven stress distribution in MBH/PVC composite when affected by external forces. Moreover, the agglomeration of MBH also resulted in less improvement in the thermal stability and flame retardancy of MBH/PVC composite. As shown in the fractured surface of MBH+MAL/PVC composite (Fig. 10d), a certain combination of MBH and MAL reduced the agglomeration of MBH, but the structure of the composite was still loose. MBH+MAL made the interior of the PVC based composites loose and the stress could not be transmitted, which was failure to maintain the mechanical properties of the composites. MBH in MBH-L/PVC composite was needle-shaped and had been broken, showing that MBH supported the tensile stress (Fig. 10e). The dispersibility of MBH in MBH-L/PVC composite was much better than that of MBH/PVC composite, which corresponds to the results of thermal stability, flame retardancy, and mechanical

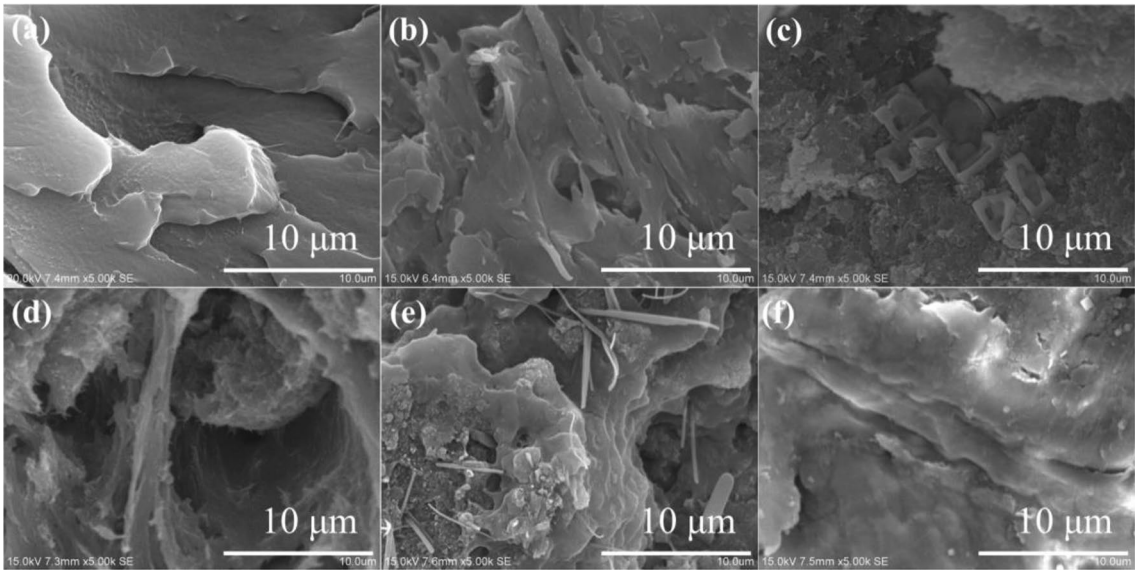

Fig. 10 SEM images of the fractured surfaces of different PVC based composites: (**a**) PVC, (**b**) MAL/PVC, (**c**) MBH/PVC, (**d**) MBH+MAL/PVC, (**e**) MBH-L/PVC, and (**f**) MBH-MAL/PVC

properties. The cross-section of MBH-MAL/PVC composite was very smooth (Fig. 10f), which is similar to that of the pure PVC. MBH, MAL, and PVC were uniformly compatible, proving that MA and in-situ synthesis could significantly increase the properties of lignin and MBH and thus promoted the fusion of MBH-MAL and PVC.

Figure 11 reveals the distribution of B and Mg elements in the PVC based composites with different additives. In the composites with in-situ synthetic additives (especially MBH-MAL/PVC), the distribution of B and Mg elements was relatively uniform, but those elements in MBH+MAL/PVC composite aggregated seriously. This is consistent with the results of SEM analysis. The aggregation of MBH in MBH+MAL/PVC composite led to the decrease in the mechanical properties of the composite, and the thermal stability and flame retardancy were also poor.

3.8 Proposed Enhancing Mechanism of In-Situ Synthesized Additives on the Properties of the Composites

A schematic diagram of the preparation processes of MBH-MAL/PVC composite is illustrated in Fig. 12a, which could be used for exploring the enhancing mechanism of in-situ synthesized additives on the properties of the composites. The particle size of lignin became smaller after MA, with looser structure and increased carboxyl and hydroxyl groups, which were favorable for in-situ synthesis of MBH. MAL with electronegative could attract Mg^{2+} during the in-situ synthesis of MBH-MAL, and the borate roots interacted with the hydrogen of the hydroxyl groups, which ensured the growth of MBH whiskers in the network of MAL. The active functional groups in the MAL interacted with the hydrogen in the PVC chain, so the MBH loaded on MAL could be uniformly combined with PVC matrix, avoiding the reunion of MBH. At the same time, the mechanical properties of PVC were hardly destroyed by the addition of MBH-MAL.

The combustion process of MBH-MAL/PVC composite is shown in Fig. 12b. When PVC was burned, HCl generated as the decomposition of PVC induced by heat. Mg^{2+} could combine with Cl^- to form $MgCl_2$, and H^+ reacted with borate roots to generated water vapor, which could take a lot of heat to cool the composites. Mg^{2+} promoted the carbonization of MAL, and part of the borate formed a glassy coating on the surface of the combustion product, which could inhibit the entry of oxygen and the escape of HCl to achieve the purpose of flame retardancy. Lignin formed char at high temperature rather than decomposed, which could effectively prevent heat transfer to the interior of the composites. Therefore, MBH-MAL can be considered as an effective additive to improve the flame retardancy and thermal stability of PVC based composites without significant decrease of the mechanical properties of PVC.

4 Conclusions

MBH-MAL complex was successfully prepared by in-situ synthesis for using as a novel additive to improve the thermal stability and flame retardancy of PVC based composites with DOP as plasticizer. A systematic investigation was also performed with MAL, MBH, MBH+MAL, and MBH-L

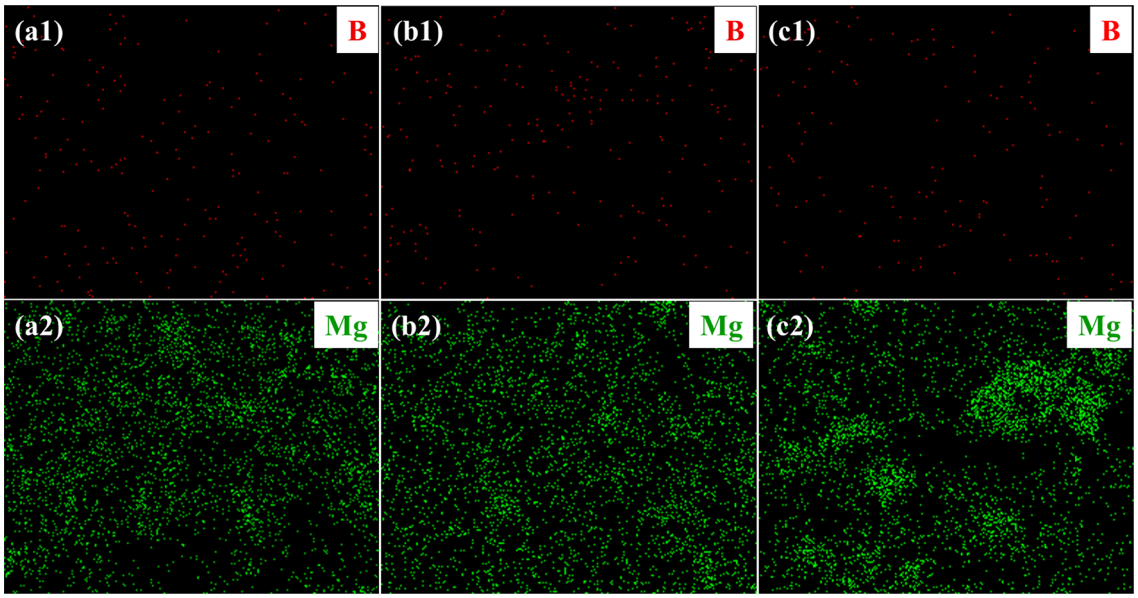

Fig. 11 EDS mapping images of different PVC based composites: (**a**) MBH-L/PVC, (**b**) MBH-MAL/PVC, and (**c**) MBH+MAL/PVC

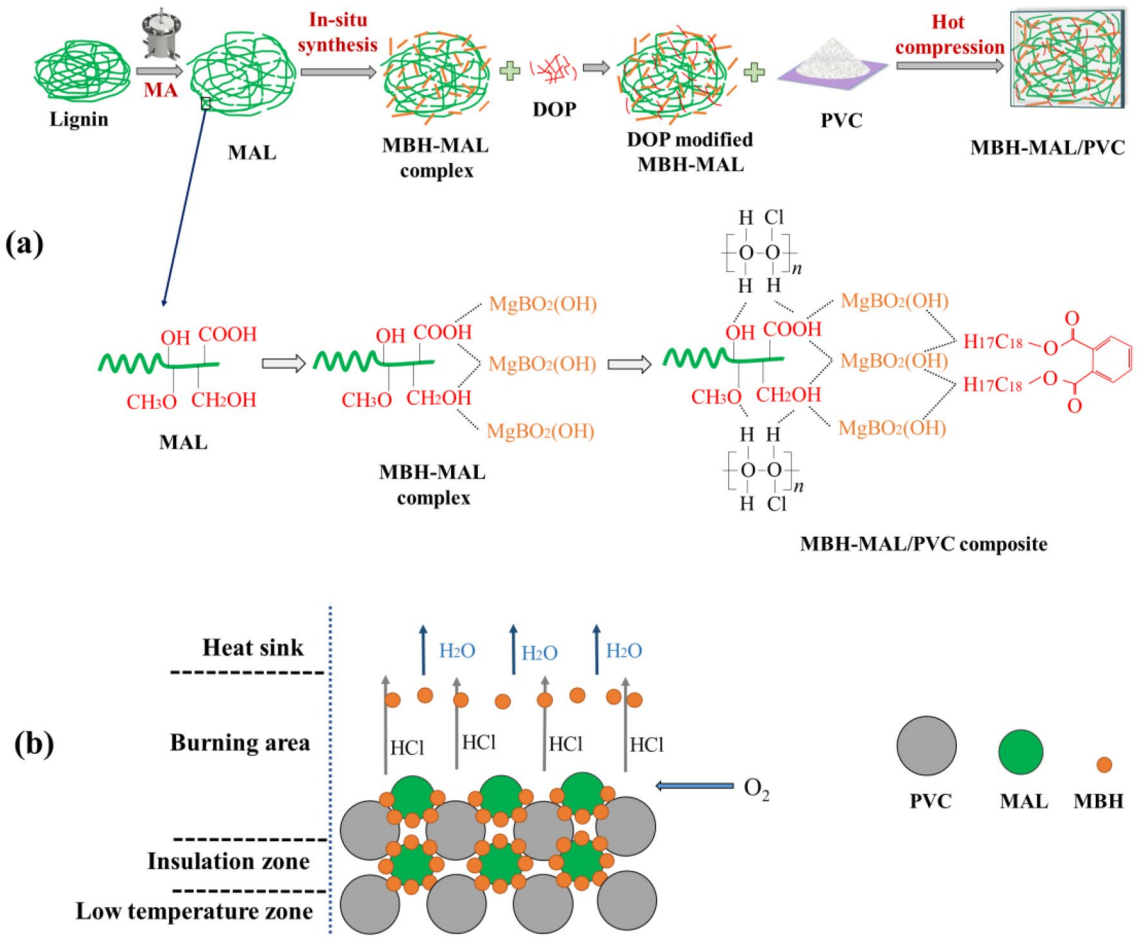

Fig. 12 Schematic diagram of (**a**) the preparation process and (**b**) the combustion process of MBH-MAL/PVC composite

used as comparative additives for preparing the composites. MBH-MAL effectively inhibited the thermal decomposition of PVC and promoted more char formation. MBH-MAL/PVC composite exhibited excellent flame retardancy and thermal stability without significant decrease of mechanical properties, ascribed to the uniformly in-situ growth of MBH in the MAL network with abundant active functional groups and the good compatibility between MBH-MAL and PVC matrix. During the combustion process of the composites, MBH could form a coating to prevent the entry of oxygen and release moisture to remove heat. MAL formed char at high temperature, which prevented the heat from transferring to the interior of the composites. Synergistic interaction of MAL and MBH in MBH-MAL complex showed excellent effect for enhancing the thermal stability and flame retardancy of PVC based composites.

Acknowledgements This research was supported by National Natural Science Foundation of China (Nos. 21666005 and 22068007), Guangxi Natural Science Foundation, China (Nos. 2017GXNSFEA198001 and 2019GXNSFDA245020), and the Scientific Research Foundation of Guangxi University, China (Grant No. XJPZ160713).

Declarations

Conflict of interest The authors declare that they have no known competing financial interests or personal relationships that could have appeared to influence the work reported in this paper.

References

1. D. Jiang, S. Zhou, Z. Fu, Q. Xu, J. Xiao, M. Zheng, W. Zhong, X. Liu, S.R. Kirk, D. Yin, Nano-silica@PVC-bonded *N*-ethyl sulfamic acid as a recyclable solid catalyst for the hydroxyalkylation of phenol with formaldehyde to bisphenol F B. Chem. Soc. Jpn. **92**, 1394–1403 (2019). https://doi.org/10.1246/bcsj.20190081
2. N. Rouabah, B. Boudine, R. Nazir, M. Zaabat, M. Sebais, O. Halimi, M.T. Soltani, A. Chala, Structural, optical and photocatalytic properties of PVC/CdS nanocomposites prepared by soft chemistry method. J. Inorg. Organomet. Polym. **31**, 1102–1110 (2021). https://doi.org/10.1007/s10904-020-01752-x
3. A. Guedri, M. Zaabat, B. Boudine, A. Hafdallah, Synthesis, Characterization, structural, and optical properties of polyvinyl chloride/zinc oxide nanocomposite films for photocatalysis application. J. Inorg. Organomet. Polym. **30**, 4884–4894 (2020). https://doi.org/10.1007/s10904-020-01604-8
4. G. Mohammed, A.M. El Sayed, S. El-Gamal, Effect of M nitrates on the optical, dielectric relaxation and porosity of PVC/PMMA membranes (M = Cd Co, Cr or Mg). J. Inorg. Organomet. Polym. **30**, 1306–1319 (2020). https://doi.org/10.1007/s10904-019-01307-9
5. W. Xie, A. Tiraferri, X. Ji, C. Chen, Y. Bai, J.C. Crittenden, B. Liu, Green and sustainable method of manufacturing anti-fouling zwitterionic polymers-modified poly(vinyl chloride) ultrafiltration membranes. J. Colloid Interface Sci. **591**, 343–351 (2021). https://doi.org/10.1016/j.jcis.2021.01.107
6. Y. Wang, X. Nie, G. Fang, L. Xiao, Synthesis and application of a novel thermostable epoxy plasticizer based on levulinic acid for poly(vinyl chloride). J. Appl. Polym. Sci. **137**, 49066 (2020). https://doi.org/10.1002/app.49066
7. J. Li, S. Jin, G. Lan, Z. Xu, L. Wang, N. Wang, L. Li, Research on the glass transition temperature and mechanical properties of poly(vinyl chloride)/dioctyl phthalate (PVC/DOP) blends by molecular dynamics simulations. Chin. J. Polym. Sci. **37**, 834–840 (2019). https://doi.org/10.1007/s10118-019-2249-5
8. Z. Wei, Y. Zhao, C. Wang, S. Kuga, Y. Huang, M. Wu, Antistatic PVC-graphene composite through plasticizer-mediated exfoliation of graphite. Chin. J. Polym. Sci. **36**, 1361–1367 (2018). https://doi.org/10.1007/s10118-018-2160-5
9. G.R. Gupta, M.R. Nevare, A.M. Patil, V.V. Gite, Unprecedented exploration of ionic liquids as additives which astonishes the thermal stability of PVC formulations. Bull. Mater. Sci. **42**, 203 (2019). https://doi.org/10.1007/s12034-019-1866-5
10. M. Dinari, N. Roghani, Calcium iron layered double hydroxide/poly(vinyl chloride) nanocomposites: synthesis, characterization and Cd^{2+} removal behavior. J. Inorg. Organomet. Polym. **30**, 808–819 (2020). https://doi.org/10.1007/s10904-019-01265-2
11. D.M. Da Silva Freitas, P.L.B. Araujo, E.S. Araujo, K.A.D.S. Aquino, Effect of copper sulfide nanoparticles in poly(vinyl chloride) exposed to gamma irradiation. J. Inorg. Organomet. Polym. **27**, 1546–1555 (2017). https://doi.org/10.1007/s10904-017-0615-8
12. Y. Gao, Q. Wang, W. Lin, Ammonium polyphosphate intercalated layered double hydroxide and zinc borate as highly efficient flame retardant nanofillers for polypropylene. Polymers **10**, 1114 (2018). https://doi.org/10.3390/polym10101114
13. T. Chan-Hom, W. Yamsaengsung, B. Prapagdee, T. Markpin, N. Sombatsompop, Flame retardancy, antifungal efficacies, and physical-mechanical properties for wood/polymer composites containing zinc borate. Fire Mater. **41**, 675–687 (2017). https://doi.org/10.1002/fam.2408
14. H.A. Raslan, M.Y. Elnaggar, E.S. Fathy, Flame-retardancy and physico-thermomechanical properties of irradiated ethylene propylene diene monomer inorganic composites. J. Vinyl Addit. Technol. **25**, 59–67 (2018). https://doi.org/10.1002/vnl.21615
15. D. Son, S. Gu, J. Choi, D.J. Suh, J. Jae, J. Choi, J. Ha, Production of phenolic hydrocarbons from organosolv lignin and lignocellulose feedstocks of hardwood, softwood, grass and agricultural waste. J. Ind. Eng. Chem. **69**, 304–314 (2019). https://doi.org/10.1016/j.jiec.2018.09.009
16. B. Ulum, S. Ilyas, A.N. Fahri, I. Mutmainna, M.A. Anugrah, N. Yudasari, E.B. Demmalino, D. Tahir, composite carbon-lignin/zinc oxide nanocrystalline ball-like hexagonal mediated from jatropha curcas L leaf as photocatalyst for industrial dye degradation. J. Inorg. Organomet. Polym. **30**, 4905–4916 (2020). https://doi.org/10.1007/s10904-020-01631-5
17. M. Yong, Y. Zhang, S. Sun, W. Liu, Properties of polyvinyl chloride (PVC) ultrafiltration membrane improved by lignin: hydrophilicity and antifouling. J. Membr. Sci. **575**, 50–59 (2019). https://doi.org/10.1016/j.memsci.2019.01.005
18. D. Feldman, D. Banu, A. El-Aghoury, Plasticization effect of lignin in some highly filled vinyl formulations. J. Vinyl Addit. Technol. **13**, 14–21 (2007). https://doi.org/10.1002/vnl.20098
19. S.S. Nisha, M. Nikzad, M. Al Kobaisi, V.K. Truong, I. Sbarski, The role of ionic-liquid extracted lignin micro/nanoparticles for functionalisation of an epoxy-based composite matrix. Compos. Sci. Technol. **174**, 11–19 (2019). https://doi.org/10.1016/j.compscitech.2019.02.009
20. W.G. Glasser, About making lignin great again-some lessons from the past. Front. Chem. **7**, 1–17 (2019). https://doi.org/10.3389/fchem.2019.00565
21. X. Zhao, Y. Zhang, H. Hu, Z. Huang, Y. Qin, F. Shen, A. Huang, Z. Feng, Effect of lignin esters on improving the thermal

properties of poly(vinyl chloride). J. Appl. Polym. Sci. **136**, 47176 (2019). https://doi.org/10.1002/app.47176
22. C. Gao, L. Zhou, S. Yao, Phosphorylated kraft lignin with improved thermal stability. Int. J. Biol. Macromol. **162**, 1642–1652 (2020). https://doi.org/10.1016/j.ijbiomac.2020.08.088
23. Y. Wang, Y. Zhang, B. Liu, A novel phosphorus-containing lignin-based flame retardant and its application in polyurethane. Compos. Commun. **21**, 100382 (2020). https://doi.org/10.1016/j.coco.2020.100382
24. Q. Yan, Z. Cai, Issues in preparation of metal-lignin nanocomposites by coprecipitation method. J. Inorg. Organomet. Polym. Mater. (2020). https://doi.org/10.1007/s10904-020-01698-0
25. A. Fourmont, S. Le Gallet, O. Politano, C. Desgranges, F. Baras, Effects of planetary ball milling on AlCoCrFeNi high entropy alloys prepared by spark plasma sintering: experiments and molecular dynamics study. J. Alloy. Compd. **820**, 153448 (2020). https://doi.org/10.1016/j.jallcom.2019.153448
26. Y. Zhang, M. Huang, J. Su, H. Hu, M. Yang, Z. Huang, D. Chen, J. Wu, Z. Feng, Overcoming biomass recalcitrance by synergistic pretreatment of mechanical activation and metal salt for enhancing enzymatic conversion of lignocellulose. Biotechnol. Biofuels **12**, 12 (2019). https://doi.org/10.1186/s13068-019-1354-6
27. Q. Li, F. Shen, Y. Zhang, Z. Huang, Y. Muhammad, H. Hu, Y. Zhu, C. Yu, Y. Qin, Graphene incorporated poly(vinyl chloride) composites prepared by mechanical activation with enhanced electrical and thermo-mechanical properties. J. Appl. Polym. Sci. **137**(7), 48375 (2019). https://doi.org/10.1002/app.48375
28. W. Zhu, L. Xiang, Q. Zhang, X. Zhang, L. Hu, S. Zhu, Morphology preservation and crystallinity improvement in the thermal conversion of the hydrothermal synthesized $MgBO_2(OH)$ nanowhiskers to $Mg_2B_2O_5$ nanowhiskers. J. Cryst. Growth **310**, 4262–4267 (2008). https://doi.org/10.1016/j.jcrysgro.2008.06.072
29. Q. Ye, X. Ma, B. Li, Z. Jin, Y. Xu, C. Fang, X. Zhou, Y. Ge, F. Ye, Development and investigation of lanthanum sulfadiazine with calcium stearate and epoxidised soyabean oil as complex thermal stabilizers for stabilizing poly(vinyl chloride). Polymers **11**, 531 (2019). https://doi.org/10.3390/polym11030531
30. A. Verma, R.K. Soni, M. Teotia, Prevention of poly(vinyl chloride) degradation through organic terephthalamides generated from poly(ethylene terephthalate) waste. J. Appl. Polym. Sci. **136**, 48022 (2019). https://doi.org/10.1002/app.48022
31. W. Wang, W. Zhang, S. Zhang, J. Li, Preparation and characterization of microencapsulated ammonium polyphosphate with UMF and its application in WPCs. Constr. Build. Mater. **65**, 151–158 (2014). https://doi.org/10.1016/j.conbuildmat.2014.04.106
32. T. Gan, Y. Zhang, Y. Chen, H. Hu, M. Yang, Z. Huang, D. Chen, A. Huang, Reactivity of main components and substituent distribution in esterified sugarcane bagasse prepared by effective solid phase reaction. Carbohydr. Polym. **181**, 633–641 (2018). https://doi.org/10.1016/j.carbpol.2017.11.102
33. L. Costes, F. Laoutid, M. Aguedo, A. Richel, S. Brohez, C. Delvosalle, P. Dubois, Phosphorus and nitrogen derivatization as efficient route for improvement of lignin flame retardant action in PLA. Eur. Polym. J. **84**, 652–667 (2016). https://doi.org/10.1016/j.eurpolymj.2016.10.003
34. H. Zhou, Y. Chang, X. Wu, D. Yang, X. Qiu, Horseradish peroxidase modification of sulfomethylated wheat straw alkali lignin to improve its dispersion performance. ACS Sustain. Chem. Eng. **3**, 518–523 (2015). https://doi.org/10.1021/sc500757y
35. F. Monteil-Rivera, L. Paquet, Solvent-free catalyst-free microwave-assisted acylation of lignin. Ind. Crop. Prod. **65**, 446–453 (2015). https://doi.org/10.1016/j.indcrop.2014.10.060
36. Z. Liao, Z. Huang, H. Hu, Y. Zhang, Y. Tan, Microscopic structure and properties changes of cassava stillage residue pretreated by mechanical activation. Bioresour. Technol. **102**, 7953–7958 (2011). https://doi.org/10.1016/j.biortech.2011.05.067
37. A.S. Kipcak, E. Moroydor Derun, S. Piskin, Magnesium borate synthesis by microwave energy: a new method. J. Chem. **2013**, 1–6 (2013). https://doi.org/10.1155/2013/329238
38. F. Ma, N. Yuan, J. Ding, The conductive network made up by the reduced graphene nanosheet/polyaniline/polyvinyl chloride. J. Appl. Polym. Sci. **128**, 3870–3875 (2013). https://doi.org/10.1002/app.38624
39. L. Dong, Y. Su, Y. Qiao, R. Li, J. Xu, Y. Chen, H. Ma, Structure regulation of boron-doped calcium hydroxystannate and its enhancement on flame retardancy and mechanical properties of PVC. Polym. Adv. Technol. **32**, 1831–1843 (2021). https://doi.org/10.1002/pat.5224
40. Y. Ning, S. Guo, Flame-retardant and smoke-suppressant properties of zinc borate and aluminum trihydrate-filled rigid PVC. J. Appl. Polym. Sci. **77**, 3119–3127 (2000). https://doi.org/10.1002/1097-4628(20000929)77:14%3c3119::AID-APP130%3e3.0.CO;2-N
41. I. Boughattas, E. Pellizzi, M. Ferry, V. Dauvois, C. Lamouroux, A. Dannoux-Papin, E. Leoni, E. Balanzat, S. Esnouf, Thermal degradation of γ-irradiated PVC: II-isothermal experiments. Polym. Degrad. Stab. **126**, 209–218 (2016). https://doi.org/10.1016/j.polymdegradstab.2015.05.010
42. W. Meng, Y. Dong, J. Li, L. Cheng, H. Zhang, C. Wang, Y. Jiao, J. Xu, J. Hao, H. Qu, Bio-based phytic acid and tannic acid chelate-mediated interfacial assembly of $Mg(OH)_2$ for simultaneously improved flame retardancy, smoke suppression and mechanical properties of PVC. Compos. Part B **188**, 107854 (2020). https://doi.org/10.1016/j.compositesb.2020.107854
43. Q. Song, H. Wu, H. Liu, T. Wang, W. Meng, H. Qu, Chitosan-regulated inorganic oxyacid salt flame retardants: preparation and application in PVC composites. J. Therm. Anal. Calorim. (2020). https://doi.org/10.1007/s10973-020-10170-7
44. A. De Chirico, M. Armanini, P. Chini, G. Cioccolo, F. Provasoli, G. Audisio, Flame retardants for polypropylene based on lignin. Polym. Degrad. Stab. **79**, 139–145 (2003). https://doi.org/10.1016/S0141-3910(02)00266-5
45. M. Bocqué, V. Lapinte, V. Courault, J. Couve, P. Cassagnau, J. Robin, Phosphonated lipids as primary plasticizers for PVC with improved flame retardancy. Eur. J. Lipid Sci. Technol. **120**, 1800062 (2018). https://doi.org/10.1002/ejlt.201800062